In-depth analysis of antifouling mechanism of the Ca^{2+}-carboxyl intra-bridging thin film composite membrane in forward osmosis

Xiujuan Hao[a], Shanshan Gao[b], Ruijun Zhang[b], Jiayu Tian[a,b,*], Yan Sun[c], Songxue Wang[a], Wenxin Shi[d], Fuyi Cui[d]

[a]State Key Laboratory of Urban Water Resource and Environment, Harbin Institute of Technology, Harbin 150090, China, Tel. +86 451 86283001; emails: tjy800112@163.com (J. Tian), hxj_hit@163.com (X. Hao), songxue.wang@outlook.com (S. Wang)
[b]School of Civil Engineering and Transportation, Hebei University of Technology, Tianjin 300401, China, Tel. +86 22 60435990; emails: gsjy_2010@163.com (S. Gao), zrj@hebut.edu.cn (R. Zhang)
[c]School of Civil Engineering, Chang'an University, Xi'an 710061, China, Tel. +86 1884589 6428; email: sunyan2021@163.com (Y. Sun)
[d]School of Environment and Ecology, Chongqing University, Chongqing 400044, China, Tel. +86 23 65120755; emails: swx@hit.edu.cn (W. Shi), cuifuyi@hit.edu.cn (F. Cui)

ABSTRACT

In this study, the fouling mechanism of the Ca^{2+}-carboxyl intra-bridging thin film composite membrane (TFC-Ca^{2+} membrane) was investigated by Extended Derjaguin–Landau–Verwey–Overbeek theory regarding the influence of organic foulant together with divalent ions, and the forward osmosis (FO) fouling experiments of the TFC-Ca^{2+} membranes were carried out by taking sodium alginate as a model foulant to represent extracellular polymeric substance in simulated seawater. Experimental results showed that the TFC-Ca^{2+} membrane had higher interfacial energy and lighter membrane fouling compared to that of TFC-control membrane (without adding Ca^{2+} in the preparation of membrane). The higher positive value of interfacial energy means repulsion between the membrane and organic foulant. According to the results of scanning electron microscope, energy dispersive X-ray spectroscopy, and total organic carbon analysis, a thin fouling layer was formed on the surface of TFC-Ca^{2+} membrane, and the fouled TFC-Ca^{2+} membrane contained a small amount of organic matters and bivalent metals. The fouling layer on the TFC-Ca^{2+} membrane was easily removed by simple physical cleaning. The results indicated that the TFC-Ca^{2+} membrane by shielding the interactions of organic matter-Ca^{2+} (in the feed solution)-membrane can effectively reduce the initial adsorption contamination, alleviate the deposition of organic foulants and mitigate the formation and the subsequent growth of fouling layer on the membrane surface. The present study is expected to provide an enlightening guide for the TFC polyamide membrane preparation, modification and fouling control.

Keywords: Forward osmosis; Fouling mechanism; Interfacial energy; Sodium alginate

1. Introduction

Membrane technology has attracted ever increasing attentions as a promising alternative to utilize unconventional water resources such as wastewater [1]. The thin-film composite (TFC) membrane, as the most advanced osmosis membrane, has been widely employed in reverse osmosis (RO) and forward osmosis (FO) membrane separation processes to produce potable water and energy [2–4].

* Corresponding author.

In particular, the FO-based wastewater treatment and water reclamation have attracted significant interests, which can simultaneously get fresh water from the diluted draw solution and recover nutrients from the concentrated feed solution [5–11]. FO has the features that greatly compromise the costs and improve energy efficiencies, thus making full use of the global water-energy nexus [10,11]. The FO process has been observed to have high fouling resistance compared to other pressure-driven membrane processes, such as nanofiltration (NF) and RO [12–15]. Nevertheless, membrane fouling is still a key issue negatively affecting TFC FO performance and efficiency [16–23].

The TFC FO membrane consists of a thin polyamide active (PA) layer and a porous support layer, in which the PA layer mainly determines the separation performance and fouling characteristics of the membrane [3,4]. As the PA layer is fabricated by interfacial polymerization (IP) between polyamine and acyl chloride monomer, a certain amount of carboxyl groups can be produced on the polyamide membrane surface [24,25]. The Ca^{2+} bridging interaction with carboxyl groups among PA layer and organic foulants is one of the major factors affecting the fouling behavior of TFC FO membrane [10,26–31]. Chemical modification or functionalization of the PA layer of TFC membranes by reacting with carrying functional groups has been widely investigated to overcome these problems [16,32–36]. For example, the incorporation of novel functional monomers [33], nanomaterials [32,36], additives [34] into the PA layer for in-situ modification, or in the aqueous/organic phase by affecting the interfacial polymerization reaction can finely tune the microstructure and morphology of resultant membranes, and in turns improve the separation performance, antifouling of as-fabricated TFC membranes. In our previous work, we designed a Ca^{2+}-intra-bridged TFC membrane (prepared by Ca^{2+} pre-occupying the carboxyl groups in the PA layer during IP process, abbreviated to TFC-Ca^{2+} membrane) and studied the membrane properties, which presented outstanding water permeation, salt rejection, and antifouling behaviors compared to conventional TFC membrane [37]. However, there is a lack of in-depth understanding of the antifouling mechanism on the TFC-Ca^{2+} membrane. According previous studies, the Extended Derjaguin–Landau–Verwey–Overbeek (XDLVO) theory was used to describe organic fouling in terms of interaction forces between organic matters and a membrane surface [38–40].

In this paper, we entirely focused on studying the fouling mechanism of the TFC-Ca^{2+} membrane by using sodium alginate as model organic foulant under the ionic strength of seawater. The fouling behaviors of the TFC-Ca^{2+} membranes were evaluated by varying the divalent ion compositions of the feed solutions in FO mode. The XDLVO theory was used to quantify the interfacial interaction energies to explain the observed fouling phenomenon. Total organic carbon (TOC) analyzer, scanning electron microscope (SEM), and energy dispersive X-ray spectroscopy (EDX) were used to characterize the fouling layer composition and thickness. The comprehensive discussion on these issues could provide novel insight on the mitigation of TFC-Ca^{2+} FO membrane fouling and achieving a high-performance TFC FO membrane.

2. Material and methods

2.1. Materials and chemicals

All chemicals and reagents used in this study were of analytical grade unless otherwise specified. Udel® polysulfone (PSf, M_n = 143 kDa, η = 1.01 dL g^{-1}) as the polymer material was obtained from Solvay. The PSf substrate were fabricated by solvent N-methyl-2-pyrrolidone (NMP, Sigma-Aldrich, Belgium, >99.5%) and pore former diethylene glycol (DEG, Sigma-Aldrich, Belgium, >99.0%). M-Phenylenediamine (MPD, Sigma-Aldrich, Belgium, >99%), and trimesoyl chloride (TMC, Sigma-Aldrich, Belgium, >98%) were employed to synthesize the polyamide active layer via interfacial polymerization. Sodium chloride (NaCl), calcium chlorides ($CaCl_2$), and magnesium chloride ($MgCl_2$) were purchased from Tianjin Kemiou Chemical Reagent Co., Ltd., China. All working solutions were prepared by using Milli-Q water with a resistivity of 18.2 MΩ cm. For membrane fouling evaluation, sodium alginate (Sigma-Aldrich, Belgium) was selected as the model organic foulant to represent polysaccharides. The stock solution of the membrane foulant was prepared by dissolving the foulants' power in Milli-Q water. All stock solutions were kept in the dark at 4°C and used within 1 month.

2.2. Interfacial energy

The interfacial energy components of the TFC membranes and foulants were determined by measuring contact angles and zeta potentials (in Table S1) between the membrane and three well-characterized probe liquids with known surface tension components. In this study, ultrapure water, diiodomethane, and DEG were used to calculate the total interfacial energy (ΔG^{TOT}) according to the described methods [33,38–40].

The ΔG^{TOT} is the sum of Lifshitz−van der Waals force (LW), acid–base (AB), and electrostatic (EL) interactions components of interfacial free energy, which describes the attraction or repulsion of solid material interacting with another solid material through a liquid medium. The detailed information of XDLVO theory can be found in the Supporting Information.

2.3. Membrane fouling experiment

Calcium-carboxyl intra-bridging TFC membranes were prepared by ourselves, in which Ca^{2+} was introduced into the MPD monomer solution before IP reaction. The details of preparation process were shown in our previous work [37]. According to our previous work, the Ca^{2+} modified TFC membrane possesses the optimal antifouling performance when the $CaCl_2$ dosage in MPD solution was 1 wt.%. Briefly, the polymer (PSf, 15 wt.%), pore former (DEG, 17 wt.%), and solvent (NMP, 68 wt.%) were mixed and stirred for 12 h for complete dissolution to prepare the PSf substrate. Then IP reaction was performed on the PSf substrate to prepare TFC membranes. The prepared membrane was stored in ultrapure water at 4°C prior to use.

The membrane fouling experiments were performed on a bench-scale cross-flow FO filtration system as illustrated in Fig. 1. The experiments were conducted using 2 L feed
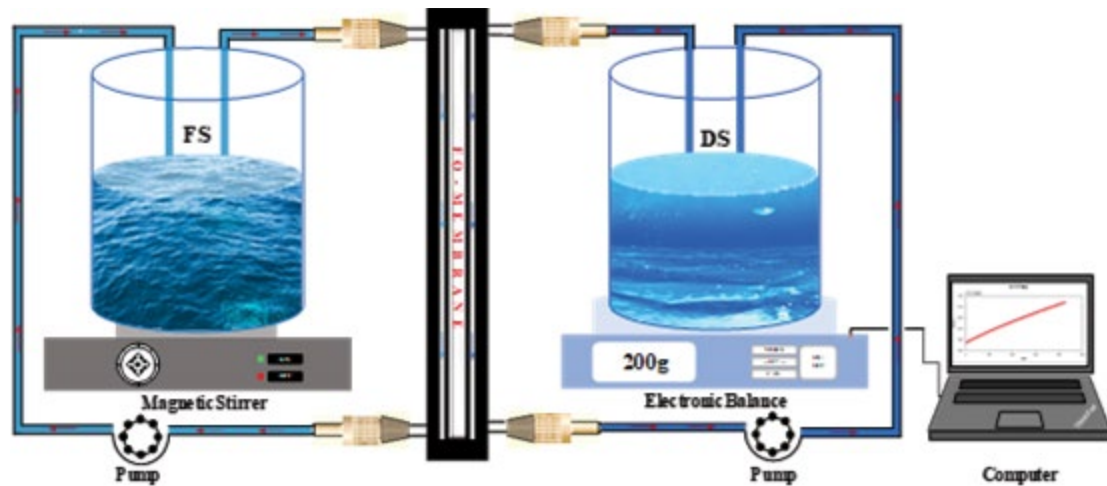
Fig. 1. Schematic diagram of the FO filtration setup used in this study.

solution containing different divalent ions (Mg^{2+}/Ca^{2+}, presented in Table 1), therefore the effect of divalent ions on the fouling propensity of sodium alginate (pH 7.0 ± 0.2, ~25°C) was investigated. To mimic seawater desalination processes, the total ionic strengths (Table 1) for feed solutions were calculated based on [41]. NaCl solution was used as draw solution, and the initial permeate flux was set at 22 ± 0.5 L/m² h (LMH) by adjusting NaCl concentration for all experiments. Both feed solution and draw solution were recirculated at a cross-flow velocity of 8.5 cm/s (Re ≈ 174) for a duration of 10 h and a new membrane coupon was used for each experiment. Prior to each fouling experiment, the baseline experiment was performed where only the background electrolytes (without foulant) were filtered for the same duration as that in the fouling experiments. The presented flux decline curves were corrected using the baseline to isolate the effect of membrane fouling. FO water flux was determined based on the weight change of draw solution in accordance to [42–44]. Each fouling experiment was repeated twice using different membrane coupons.

2.4. Membrane cleaning

Membrane cleaning was performed immediately at the end of the fouling test to evaluate the reversibility of membrane fouling. The fouled membrane was cleaned with ultrapure water at a fixed cross-flow velocity of 8.5 cm/s for 60 min. After cleaning, the feed solution without sodium alginate was then used to measure the water

flux thus calculating the flux recovery ratio. Each cleaning experiment was repeated twice using different membrane coupons.

2.5. Characterization of fouled membranes

To determine the content of organic matters on the fouled membrane surfaces, membrane coupons with an area of 2.0 cm × 2.0 cm were soaked in 20 mL ultrapure water at 4°C. The dissolved water samples were collected and the amount of TOC was quantified by TOC analyzer (TOC-5000A, Shimadzu, Japan). The average values from two membrane samples were reported. The structure morphologies of fouled membranes were analyzed by an SEM (Model XL 30, Philips, Netherlands), which was equipped with an EDX [19,21,24]. The fouled membranes were dried in a vacuum at room temperature (25°C) for 24 h. For cross-section analysis, the membranes were fractured into small pieces after immersing in liquid nitrogen for 5 min. Then the membrane samples were sputter-coated with a thin layer of gold. EDX analysis was used to quantify the element composition on the fouled membrane surfaces. The basic characteristics of the fouling layer could be observed, then the comparison of the fouling extent between TFC-control membranes and TFC-Ca^{2+} membranes could be made. To XDLVO analysis, Zeta potentials of the model foulant solutions were examined via the Zetasizer instrument (Zetasizer Nano series Nano-ZS90, Malvern Panalytical, British and Holland), contact angles of the foulants and membranes were determined

Table 1
List of the different feed solutions and their compositions

Feed solution (FS)	FS composition	Osmotic pressure (bar)	Total ionic strength (mM)
Solution 1	350 mM NaCl + 50 mM MgCl$_2$	0.40	
Solution 2	476 mM NaCl + 8 mM CaCl$_2$	0.48	500 mM
Solution 3	326 mM NaCl + 50 mM MgCl$_2$ + 8 mM CaCl$_2$	0.39	

by contact angle goniometer (SL200B, Solon Tech Co., Ltd., China). The probe liquids for contact angle measurement were ultrapure water, glycerol, and diiodomethane. All of the above experiments were repeated twice.

3. Results and discussion

3.1. Interfacial energy between membrane and foulant

To explain the complex property of TFC polyamide membrane surface combined with solidum alginate, the XDLVO prediction method was introduced to analyze the interactions between the polyamide membrane and sodium alginate at the minimum distance (d_0 = 0.158 nm). Membrane-foulant interfacial energies provide information about the interaction of a clean membrane with foulants in feed solution and about the likelihood of initial adsorption of foulants to the membrane surface [39,41,46,47]. Positive value of interfacial energy between membrane and foulant signifies a stronger resistance to membrane fouling, while negative value signifies more attractive effect between membrane surface and foulant, which would aggravate membrane fouling [38,39,48,49]. It was found that all the interfacial energies were negative values of the TFC-control membrane (Table 2), meaning high potential of membrane fouling on TFC-control membrane. For example, the TFC-control membrane exhibited the most negative energy of –37.59 mJ m^{-2} and experienced a more severe organic fouling as Mg^{2+} and Ca^{2+} simultaneously presented in the feed solution (3.2. Membrane fouling). On contrast, the corresponding interfacial energies for the TFC-Ca^{2+} membranes were varying from 11.91 to –9.43 mJ m^{-2}, indicating repulsive interactions between the TFC-Ca^{2+} membranes and foulants. The AB interaction was observed as the primary factor in the membrane-foulant interactions. The role of EL was negligible at high ionic strength (i.e., seawater) due to the electrostatic shielding effect [12]. It has been proved that van der Waals force (LW) has a lower contribution to the attraction of different solid materials, compared with the short-range acid-base (AB) interaction [38,39]. Yin et al. [50] have reported that initial fouling was dominant in seawater desalination process, the TFC-Ca^{2+} membranes with higher interfacial energy means less initial adsorption of foulants to the membrane surface. The sodium alginate and divalent ions (especially Ca^{2+}) can interact with the carboxyl group in the TFC membrane and produce serious membrane fouling. According to our previous study on the surface characteristics of TFC-Ca^{2+} membrane, the TFC-Ca^{2+} membrane contains fewer carboxylic groups in the PA layer than

TFC-control membrane, a decrease in carboxylic groups in TFC polyamide membrane would be beneficial to reduce initial bridging with Ca^{2+} and mitigate membrane-foulant interactions. The Ca^{2+} bridging interactions were reduced between TFC-Ca^{2+} membrane surface and sodium alginate, and the initial membrane−foulant interactions were weakened, thus decreasing the continuous formation and growth of a cross-linked sodium alginate gel layer on the membrane surface [51].

3.2. Membrane fouling

Fig. 2 presents the average water flux of the TFC-control membrane and the TFC-Ca^{2+} modified membrane using a feed solution containing 200 mg/L sodium alginate and different divalent ions (Mg^{2+}/Ca^{2+}, the total ionic strength of 500 mM) in feed solution. An initial flux of 22 LMH was used for the fouling experiments by adjusting the draw solution concentrations. The results clearly showed that the membrane fouling caused by sodium alginate on TFC-control membrane was more severe than that on TFC-Ca^{2+} membrane (Fig. 2), in which the highest recorded permeate flux declines were 41.7% vs. 26.3% for TFC-control membrane and TFC-Ca^{2+} membrane, as the feed solutions simultaneously contained Ca^{2+} and Mg^{2+}. From Figs. 2a and b, it can be found that the membrane suffered a higher extent of flux decline with the addition of Ca^{2+} in the feed solution than the addition of Mg^{2+} at mimic seawater level ionic strength. Particularly, a slightly more flux decline was recorded as the combined presence of Mg^{2+} and Ca^{2+} in the feed solution than that of single Ca^{2+} in the feed solution (Fig. 2c). Due to the great importance of abundant carboxyl groups on the polyamide membrane, divalent ions (particularly Ca^{2+}) had the ability to bind to the carboxyl groups of sodium alginate and polyamide surface in a uniquely arranged manner, thus leading to a highly arranged sodium alginate- Mg^{2+}/Ca^{2+}-membrane gel networks on TFC membrane surface and hence severe fouling [41,45]. In addition, the flux declines mainly happened at the early stage of fouling. These observed flux declines for TFC-Ca^{2+} membrane in the presence of divalent ions were well-correlated to the interaction of foulant-membrane according to XDLVO analysis. As the operation time increases, more significant water permeate flux reduction was observed on the TFC-control membrane system. The results also supported the findings that the incorporation of Ca^{2+} during membrane preparation decreased the surface carboxyl group sites and led to less Ca^{2+} bridge-formation between sodium alginate and the TFC-Ca^{2+} polyamide membrane surface.

Table 2
XDLVO for interaction energy predictions of TFC-control membrane-foulant or TFC-Ca^{2+} modified membrane-foulant system in the various salt solutions (unit: mJ m^{-2})

	r^{LW}	r^+	r^-	r^{TOT}	TFC-control membrane				TFC-Ca^{2+} membrane			
					ΔG^{LW}	ΔG^{AB}	ΔG^{EL}	ΔG^{TOT}	ΔG^{LW}	ΔG^{AB}	ΔG^{EL}	ΔG^{TOT}
Solution 1	37.99	1.43	27.02	50.42	–4.24	–10.48	–0.0004	–14.72	–3.51	15.42	–0.0001	11.91
Solution 2	37.18	2.20	19.49	50.26	–4.05	–17.35	–0.0006	–21.40	–3.35	8.26	–0.0001	4.91
Solution 3	38.54	3.04	7.45	48.05	–4.37	–33.22	–0.0010	–37.59	–3.61	–5.82	–0.0009	–9.43
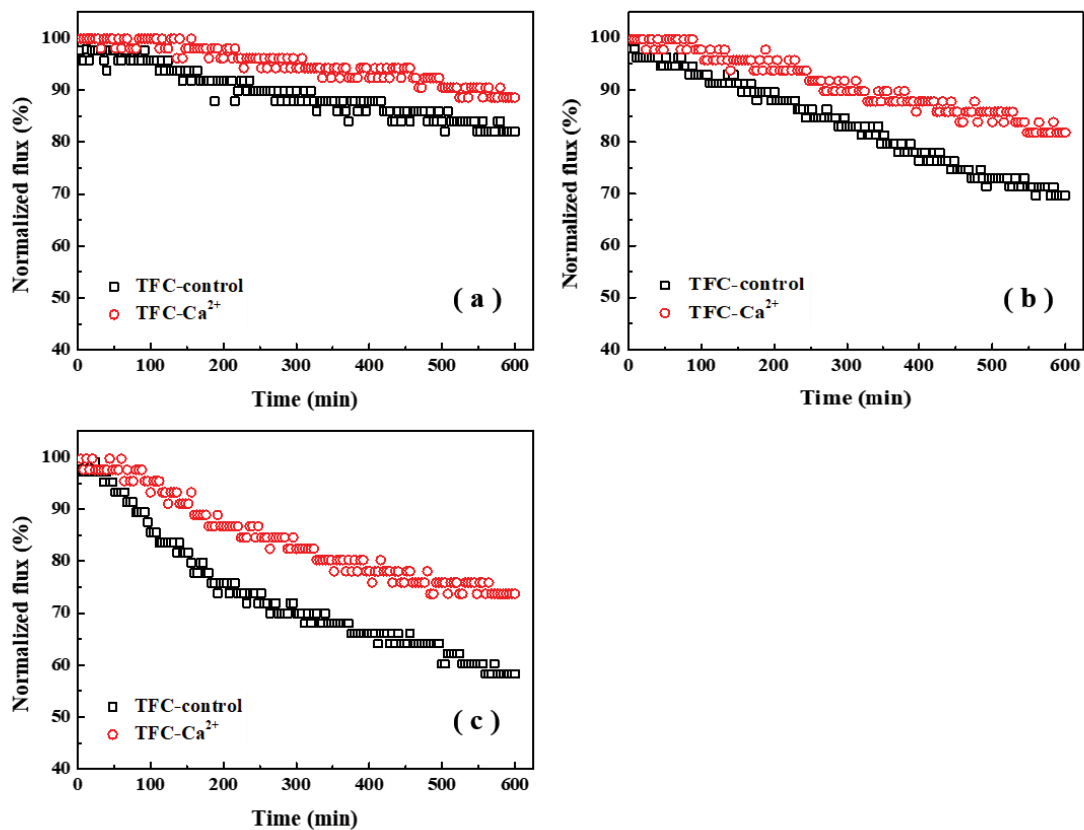
Fig. 2. Flux performance of the TFC-control and the TFC-Ca^{2+} modified membranes using sodium alginate (200 mg/L) in the presence of divalent ions (a) solution 1, $c(Ca^{2+})$ = 8 mM; (b) solution 2, $c(Mg^{2+})$ = 50 mM; (c) solution 3, $c(Ca^{2+})$ = 8 mM and $c(Mg^{2+})$ = 50 mM. An identical initial water flux of 22 LMH was used for all fouling experiments.

3.3. Membrane fouling layer characterization

For better understanding, the membrane fouling behavior in TFC-control membrane and TFC-Ca^{2+} membrane, the morphology and element composition of the fouled membranes were immediately examined by SEM and EDX at the end of fouling experiment as illustrated in Figs. 3 and 4. Based on the cross-section observation of the fouled membranes, it was clearly seen that a dense sodium alginate-Mg^{2+}/Ca^{2+}gel fouling layers were covered on the TFC-control membrane surface (Figs. 3a–c). On the contrary, a rather thin fouling layer was formed on the TFC-Ca^{2+} modified membrane surface in all scenarios with different ion compositions in feed solution (Figs. 3d–f). The thicknesses of the fouling layers on the TFC-control membrane and TFC-Ca^{2+} modified membrane with the feed solution containing both Mg^{2+} and Ca^{2+} were 25.72 ± 1.80 μm (Fig. 3c) vs. 12.23 ± 0.32 μm (Fig. 3f).

Furthermore, the EDX analysis qualitatively demonstrated that both Mg and Ca elements deposited in the fouling layer (Fig. 4). It was notable that a higher relative weight percentage of Mg/Ca deposited in the fouling layer of TFC-control membrane. The relative weight percentage of Mg/Ca was significantly reduced in the fouling layer of TFC-Ca^{2+} modified membranes, indicating the occurrence of more severe fouling on the TFC-control polyamide membrane surfaces.

The amount of foulants extracted from the organic-fouled TFC-control and TFC-Ca^{2+} membrane surfaces were analyzed by TOC after the fouling experiment. It was obvious that a significant amount of foulants were detected on the TFC-control membrane surface as shown in Fig. 5, especially in the presence of Ca^{2+}. However, the concentrations of organic matters on the fouled TFC-Ca^{2+} membranes were much lower, which was consistent with the observation of SEM and EDX analysis (Figs. 3 and 4). As well discussed in previous studies, the fouling layer formed on the membrane surface could severely lower mass transfer coefficient and directly decrease water permeability [22] and result in the severer water flux decline. The ever-growing fouling layer inevitably induces more serious gel-layers and facilitates the enrichment of organic matters on membrane surfaces.

The foulant deposition amount on the TFC-control and TFC-Ca^{2+} membrane surfaces, as well as the element contents observed from EDX results, were mostly consistent with the variations of the flux curves (Fig. 2). Based on the above discussion, it can be concluded that a bountiful supply of carboxyl groups on the TFC-control membrane is straightforwardly caused much more organic foulants accumulated on the membrane surface, this thick layer provides resistance to water permeance, resulting in the severer membrane fouling and a higher overall flux decline during the water treatment/reclamation. In contrast, the novel Ca^{2+} preoccupation strategy during the IP process by sequestrating their
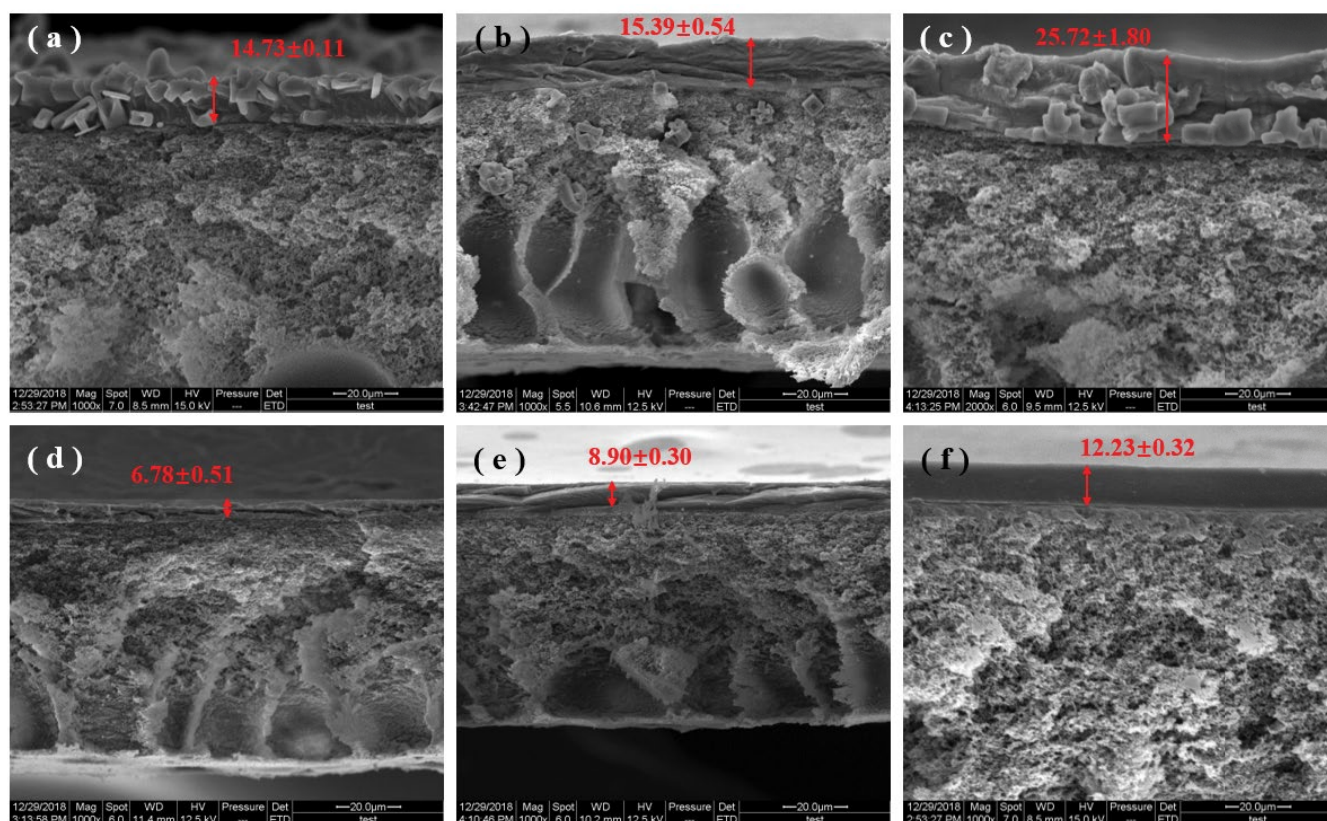
Fig. 3. SEM images of the fouled TFC-control membranes (a–c) and TFC-Ca^{2+} modified membranes (d–f). (a,d) Solution 1; (b,e) solution 2; (c,f) solution 3.
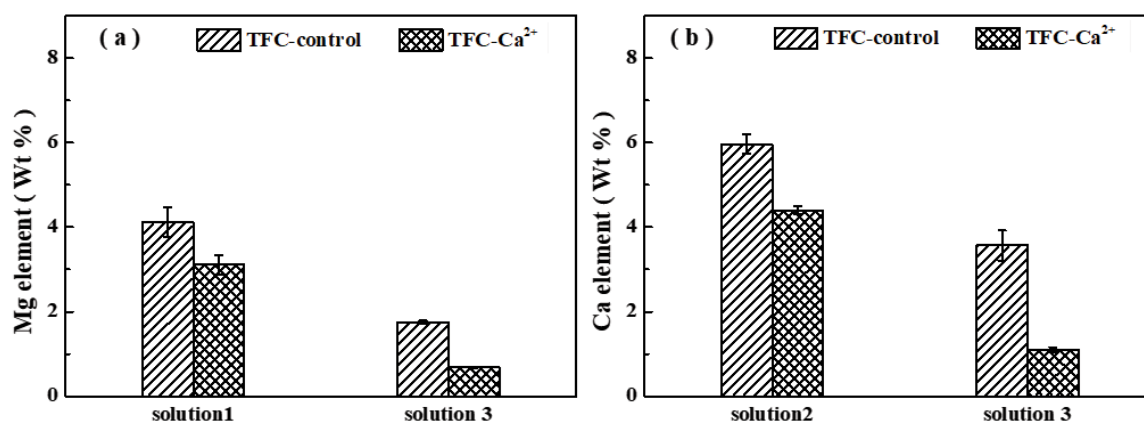
Fig. 4. EDX analysis of the element compositions on the fouled TFC-control membranes and TFC-Ca^{2+} modified membranes in different divalent ion as feed solutions.

carboxyl groups could resist the attachment of sodium alginate on the polyamide membrane surface.

3.4. Fouling reversibility

Flux recovery experiments were carried out immediately following the fouling experiments for each membrane sample to assess the fouling reversibility of TFC-control membrane and TFC-Ca^{2+} membrane, as is shown in Fig. 6. It was noticed that the TFC-Ca^{2+} modified membrane showed

higher cleaning efficiency and achieved higher water flux recovery than TFC-control membrane (Fig. 6b). The water recovery rates were 79.4% (TFC-control) and 89.9% (TFC-Ca^{2+}), respectively, under the most severe membrane fouling circumstance. This demonstrated that the membrane fouling occurred in TFC-control membrane was obviously severer than that in TFC-Ca^{2+} membrane. A more reversible fouling layer formed on the TFC-Ca^{2+} modified membrane that can be easily broken apart and removed by simple physical cleaning.
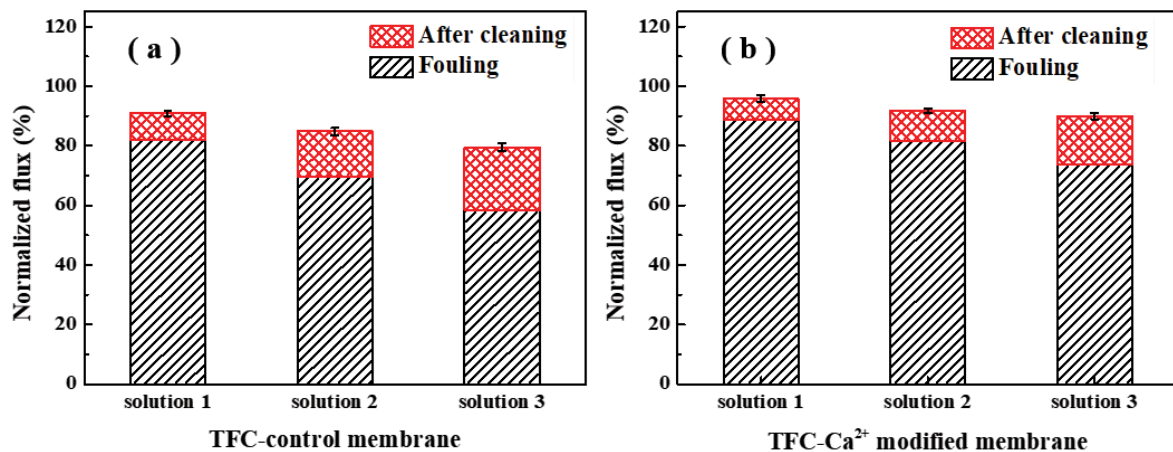
Fig. 6. Membrane fouling reversibility for the TFC-control membranes (a) and the TFC-Ca²⁺ membranes and (b) in the presence of divalent ions. Fouling reversibility was evaluated by cleaning the fouling membranes with DI water under crossflow conditions.
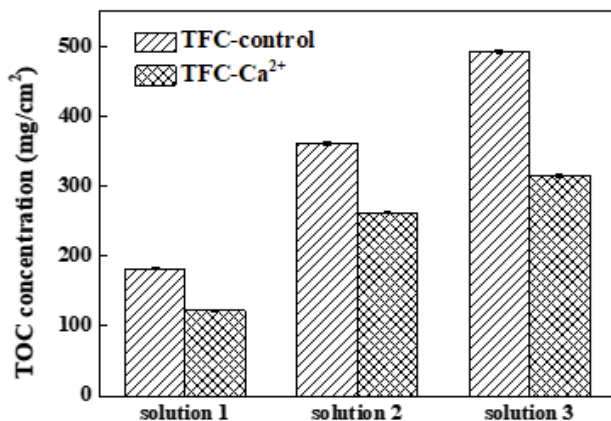
Fig. 5. The amount of organic foulant deposition on the fouled TFC-control membrane and TFC-Ca²⁺ membranes were analyzed by TOC after the fouling experiment.

4. Conclusion

The fouling mechanisms of the TFC-Ca²⁺ membrane and the influence of divalent ions were investigated by XDLVO theory and FO fouling experiments. The TFC-Ca²⁺ membrane PA layer was more resistant toward sodium alginate aggregates settling compared to the visibly thick fouling layer noticed on the TFC-control membrane. Probing the membrane-foulant interactions elucidated that there was strong repulsion between the TFC-Ca²⁺ membrane and foulants. The results of interaction energy are in striking agreement with the fouling properties of the membranes. This was due to changes in the membrane surface, which reduced the chance of membrane surface carboxyl group chelating with divalent ions, resulting in the reduction of initial fouling and the deposition of organic foulants on the membrane surface. This knowledge and the in-depth understanding of the specific ion interactions between membrane and foulants can provide a different insight into organic fouling controlling strategies of TFC polyamide membrane. Sequestration of a specific interaction between membrane surface and organic foulant is promising for lower the membrane-foulant interaction and the fouling propensity of TFC polyamide membrane.

References

[1] C.Y. Tang, Z. Yang, H. Guo, J.J. Wen, L.D. Nghiem, E. Cornelissen, Potable water reuse through advanced membrane technology, Environ. Sci. Technol., 52 (2018) 10215–10223.

[2] N. Misdan, W.J. Lau, A.F. Ismail, Seawater Reverse Osmosis (SWRO) desalination by thin-film composite membrane-current development, challenges and future prospects, Desalination, 287 (2012) 228–237.

[3] K. Lutchmiah, A.R.D. Verliefde, K. Roest, L.C. Rietveld, E.R. Cornelissen, Forward osmosis for application in wastewater treatment: a review, Water Res., 58 (2014) 179–197.

[4] L. Chekli, S. Phuntsho, J.E. Kim, J. Kim, J.Y. Choi, J. Choi, S. Kim, J.H. Kim, S. Hong, J. Sohn, H.K. Shon, A comprehensive review of hybrid forward osmosis systems: performance, applications and future prospects, J. Membr. Sci., 497 (2016) 430–449.

[5] S. Zhao, L. Zou, C.Y. Tang, D. Mulcahy, Recent developments in forward osmosis: opportunities and challenges, J. Membr. Sci., 396 (2012) 1–21.

[6] M. Guizania, M. Saitod, R. Itoa, N. Funamizue, Combined FO and RO system for the recovery of energy from wastewater and the desalination of seawater, Desal. Water Treat., 154 (2019) 14–20.

[7] J. Zhao, S. Pan, Q. Tu, H. Zhu, X. Gao, P. Zhang, Fouling characterization of TFC forward osmosis membrane in a novel dynamic sludge anaerobic digestion reactor, Desal. Water Treat., 107 (2018) 10–19.

[8] H. Zhang, W. Jiang, H. Cui, Performance of anaerobic forward osmosis membrane bioreactor coupled with microbial electrolysis cell (AnOMEBR) for energy recovery and membrane fouling alleviation, Chem. Eng. J., 321 (2017) 375–383.

[9] Y. Gao, Z. Fang, P. Liang, X. Huang, Direct concentration of municipal sewage by forward osmosis and membrane fouling behavior, Bioresour. Technol., 247 (2018) 730–735.

[10] Z. Li, V. Yangali-Quintanilla, R. Valladares-Linares, Q. Li, T. Zhan, G. Amy, Flux patterns and membrane fouling propensity during desalination of seawater by forward osmosis, Water Res., 46 (2012) 195–204.

[11] A.J. Ansari, F.I. Hai, W.E. Price, J.E. Drewes, L.D. Nghiem, Forward osmosis as a platform for resource recovery from municipal wastewater - a critical assessment of the literature, J. Membr. Sci., 529 (2017) 195–206.

[12] C.Y. Tang, T.H. Chong, A.G. Fane, Colloidal interactions and fouling of NF and RO membranes: a review, Adv. Colloid Interfaces, 164 (2011) 126–143.

[13] Q. She, R. Wang, A.G. Fane, C.Y. Tang, Membrane fouling in osmotically driven membrane processes: a review, J. Membr. Sci., 499 (2016) 201–233.

[14] M. Xie, J. Lee, L.D. Nghiem, M. Elimelech, Role of pressure in organic fouling in forward osmosis and reverse osmosis, J. Membr. Sci., 493 (2015) 748–754.

[15] E.W. Tow, M.M. Rencken, J.H. Lienhard, In situ visualization of organic fouling and cleaning mechanisms in reverse osmosis and forward osmosis, Desalination, 399 (2016) 138–147.

[16] B. Mi, M. Elimelech, Chemical and physical aspects of organic fouling of forward osmosis membranes, J. Membr. Sci., 320 (2008) 292–302.

[17] J. Li, Z. Ni, Z. Zhou, Y. Hu, X. Xu, L. Cheng, Membrane fouling of forward osmosis in dewatering of soluble algal products: comparison of TFC and CTA membranes, J. Membr. Sci., 552 (2018) 213–221.

[18] W.C.L. Lay, J. Zhang, C. Tang, R. Wang, Y. Liu, A.G. Fane, Factors affecting flux performance of forward osmosis systems, J. Membr. Sci., 394–395 (2012) 151–168.

[19] N.M. Mazlan, P. Marchetti, H.A. Maples, B. Gu, S. Karan, A. Bismarck, A.G. Livingston, Organic fouling behaviour of structurally and chemically different forward osmosis membranes–a study of cellulose triacetate and thin film composite membranes, J. Membr. Sci., 520 (2016) 247–261.

[20] Y. Sun, J. Tian, L. Song, S. Gao, W. Shi, F. Cui, Dynamic changes of the fouling layer in forward osmosis based membrane processes for municipal wastewater treatment, J. Membr. Sci., 549 (2018) 523–532.

[21] H. Wang, X. Wang, F. Meng, X. Li, Y. Ren, Q. She, Effect of driving force on the performance of anaerobic osmotic membrane bioreactors: new insight into enhancing water flux of FO membrane via controlling driving force in a two-stage pattern, J. Membr. Sci., 569 (2019) 41–47.

[22] Y. Sun, S. Gao, J. Tian, X. Hao, Z. Liu, W. Shi, F. Cui, Air bubbling for membrane fouling control in a submerged direct forward osmosis system for municipal wastewater treatment, Environ. Sci. Water Res. Technol., 5 (2019) 684–692.

[23] N.H. Ab Hamid, L. Ye, D.K. Wang, S. Smart, E. Filloux, T. Lebouteiller, X. Zhang, Evaluating the membrane fouling formation and chemical cleaning strategy in forward osmosis membrane filtration treating domestic sewage, Environ. Sci. Water Res. Technol., 4 (2018) 213–292.

[24] Y. Mo, A. Tiraferri, N.Y. Yip, A. Adout, X. Huang, M. Elimelech, Improved antifouling properties of polyamide nanofiltration membranes by reducing the density of surface carboxyl groups, Environ. Sci. Technol., 46 (2012) 13253–13261.

[25] A. Tiraferri, M. Elimelech, Direct quantification of negatively charged functional groups on membrane surfaces, J. Membr. Sci., 389 (2012) 499–508.

[26] B. Mi, M. Elimelech, Organic fouling of forward osmosis membranes: fouling reversibility and cleaning without chemical reagents, J. Membr. Sci., 348 (2010) 337–345.

[27] A Tiraferri, Y. Kang, E.P. Giannelis, M. Elimelech, Superhydrophilic thin-film composite forward osmosis membranes for organic fouling control: fouling behavior and antifouling mechanisms, Environ. Sci. Technol., 46 (2012) 11135–11144.

[28] K. Katsoufidou, S.G. Yiantsios, A.J. Karabelas, Experimental study of ultrafiltration membrane fouling by sodium alginate and flux recovery by backwashing, J. Membr. Sci., 300 (2007) 137–146.

[29] E. Arkhangelsky, F. Wicaksana, C. Tang, A.A. Al-Rabiah, S.M. Al-Zahrani, R. Wang, Combined organic–inorganic fouling of forward osmosis hollow fiber membranes, Water Res., 46 (2012) 6329–6338.

[30] L. Li, X. Wang, M. Xie, Z. Wang, X. Li, Y. Ren, In situ extracting organic-bound calcium: a novel approach to mitigating organic fouling in forward osmosis treating wastewater via gradient diffusion thin-films, Water Res., 156 (2019) 102–109.

[31] L. Li, X. Wang, M. Xie, H. Wang, X. Li, Y. Ren, EDTA-based adsorption layer for mitigating FO membrane fouling via in situ removing calcium binding with organic foulants, J. Membr. Sci., 578 (2019) 95–102.

[32] A. Zirehpour, A. Rahimpour, M. Ulbricht, Nano-sized metal organic framework to improve the structural properties and desalination performance of thin film composite forward osmosis membrane, J. Membr. Sci., 531 (2017) 59–67.

[33] Y. Wang, X. Li, C. Cheng, Y. He, J. Pan, T. Xu, Second interfacial polymerization on polyamide surface using aliphatic diamine with improved performance of TFC FO membranes, J. Membr. Sci., 498 (2016) 30–38.

[34] X. Zhang, J. Tian, S. Gao, Z. Zhang, F. Cui, C.Y. Tang, In situ surface modification of thin film composite forward osmosis membranes with sulfonated poly(arylene ether sulfone) for anti-fouling in emulsified oil/water separation, J. Membr. Sci., 527 (2017) 26–34.

[35] Y. Wu, X. Wang, Z. Wang, F. Yan, F. Zu, H. Zhang, A novel method for measuring cake porosity by ions detection technique in a conventional coagulation-ultrafiltration process, Sep. Purif. Technol., 220 (2019) 320–327.

[36] C. Liu, J. Lee, C. Small, J. Ma, M. Elimelech, Comparison of organic fouling resistance of thin-film composite membranes modified by hydrophilic silica nanoparticles and zwitterionic polymer brushes, J. Membr. Sci., 544 (2017) 135–142.

[37] X. Hao, S. Gao, J. Tian, Y. Sun, F. Cui, C.Y. Tang, Calcium-carboxyl intra-bridging during interfacial polymerization: a novel strategy to improve antifouling performance of thin film composite membranes, Environ. Sci. Technol., 53 (2019) 4371–4379.

[38] T. Lin, Z. Lu, W. Chen, Interaction mechanisms and predictions on membrane fouling in an ultrafiltration system, using the XDLVO approach, J. Membr. Sci., 461 (2014) 49–58.

[39] T. Lin, Z. Lu, W. Chen, Interaction mechanisms of humic acid combined with calcium ions on membrane fouling at different conditions in an ultrafiltration system, Desalination, 357 (2015) 26–35.

[40] C.J. Van Oss, Acid-base interfacial interactions in aqueous media, Colloid Surf., A, 78 (1993) 1–49.

[41] M.M. Motsa, B.B. Mamba, A.D Haese, E.M.V. Hoek, A.R.D. Verliefde, Organic fouling in forward osmosis membranes: the role of feed solution chemistry and membrane structural properties, J. Membr. Sci., 460 (2014) 99–109.

[42] H. Zhao, S. Qiu, L. Wu, L. Zhang, H. Chen, C. Gao, Improving the performance of polyamide reverse osmosis membrane by incorporation of modified multi-walled carbon nanotubes, J. Membr. Sci., 450 (2014) 249–256.

[43] R.V. Linares, V. Yangali-Quintanilla, Z. Li, G. Amy, NOM and TEP fouling of a forward osmosis (FO) membrane: foulant identification and cleaning, J. Membr. Sci., 421 (2012) 217–224.

[44] Y. Liu, B. Mi, Combined fouling of forward osmosis membranes: synergistic foulant interaction and direct observation of fouling layer formation, J. Membr. Sci., 407 (2012) 136–144.

[45] K. Xiao, X. Wang, X. Huang, T.D. Waite, X. Wen, Combined effect of membrane and foulant hydrophobicity and surface charge on adsorptive fouling during microfiltration, J. Membr. Sci., 373 (2011) 140–151.

[46] Y. Ding, Y. Tian, Z. Li, H. Wang, L. Chen, Microfiltration (MF) membrane fouling potential evaluation of protein with different ion strengths and divalent cations based on extended DLVO theory, Desalination, 331 (2013) 62–68.

[47] P. van den Brink, A. Zwijnenburg, G. Smith, H. Temmink, M. van Loosdrecht, Effect of free calcium concentration and ionic strength on alginate fouling in cross-flow membrane filtration, J. Membr. Sci., 345 (2009) 207–216.

[48] J.A. Brant, A.E. Childress, Assessing short-range membrane–colloid interactions using surface energetics, J. Membr. Sci., 203 (2002) 257–273.

[49] Y. Wang, C.Y. Tang, Protein fouling of nanofiltration, reverse osmosis, and ultrafiltration membranes-the role of hydrodynamic conditions, solution chemistry, and membrane properties, J. Membr. Sci., 376 (2011) 275–282.

[50] W. Yin, X. Li, S.R. Suwarno, E.R. Cornelissen, T.H. Chong, Fouling behavior of isolated dissolved organic fractions from seawater in reverse osmosis (RO) desalination process, Water Res., 159 (2019) 385–396.

[51] Y. Gu, Y. Wang, J. Wei, C.Y. Tang, Organic fouling of thin-film composite polyamide and cellulose triacetate forward osmosis membranes by oppositely charged macromolecules, Water Res., 47 (2013) 1867–1874.

Supporting information

S1. XDLVO theory analysis

The total interaction energy ΔG^{TOT} between solid materials can be determined by including the Lifshitz-van der Waals (LW) interaction ΔG^{LW}, electrostatic double layer (EL) interaction ΔG^{EL}, and Lewis acid-base (AB) interaction ΔG^{AB}, which can be expressed as follow [1,2]:

$$\Delta G^{TOT} = \Delta G^{LW} + \Delta G^{EL} + \Delta G^{AB} \tag{S1}$$

$$\Delta G^{LW} = 2\left(\sqrt{\gamma_l^{LW}} - \sqrt{\gamma_m^{LW}}\right)\left(\sqrt{\gamma_c^{LW}} - \sqrt{\gamma_l^{LW}}\right) \tag{S2}$$

$$\Delta G^{AB} = 2\sqrt{\gamma_l^+}\left(\sqrt{\gamma_m^-} + \sqrt{\gamma_c^-} - \sqrt{\gamma_l^-}\right) + \\ 2\sqrt{\gamma_l^-}\left(\sqrt{\gamma_m^+} + \sqrt{\gamma_c^+} - \sqrt{\gamma_l^+}\right) - 2\left(\sqrt{\gamma_m^+\gamma_c^-} + \sqrt{\gamma_m^-\gamma_c^+}\right) \tag{S3}$$

$$\Delta G^{EL} = \frac{\varepsilon_0\varepsilon_r\kappa}{2}\left(\zeta_m^2 + \zeta_c^2\right) \times \left(1 - \coth\left(\kappa y\right) + \frac{2\zeta_m\zeta_c}{\zeta_m^2 + \zeta_c^2}\operatorname{csch}\left(\kappa y\right)\right) \tag{S4}$$

where the subscript of m and c correspond to membrane and organic foulant, respectively. $\varepsilon_0\varepsilon_r$ is the dielectric permittivity of the fluid (i.e., $\varepsilon_0 = 8.85419 \times 10^{-12}$, $\varepsilon_r = 78$, respectively), ζ_m and ζ_c are the surface potentials of the membrane and organic foulant which were determined by zeta potential measurements, respectively. κ is the inverse Debye screening length.

Table S1
Zeta potentials and contact angles with the different feed salt solutions

	Zeta potential (mV)	Contact angle (°)
Solution 1	−11.30	47.34
Solution 2	−14.57	53.12
Solution 3	−6.36	65.37

References

[1] C.J. Van Oss, Interfacial Forces in Aqueous Media, CRC Press, Taylor & Francis, 2006.

[2] M. Hermansson, The DLVO theory in microbial adhesion, Colloids Surf., B, 14 (1999) 105–119.